Appendix 1: Internucleosomal Interaction Pattern

We sketch here how the $(i, i \pm 4)$ internucleosomal interaction pattern follows from the mean angle of approximately 90° subtended between nucleosome triplets within our oligonucleosomes using a highly simplified model of chromatin.

Consider each nucleosome core as a point object connected by straight linker DNAs. We impose only two constraints: (*i*) the angle between consecutive linker DNAs obeys a Gaussian distribution with a certain mean and variance, and (*ii*) three consecutive linker DNAs have a torsion angle in the range $[-\pi/2, \pi/2]$ to promote a helical nucleosome arrangement (see Fig. 1.1). We generate a chromatin fiber with a given number of nucleosomes N by successively adding $N-1$ linker DNAs in turn such that the angle between consecutive linker DNAs is selected from a Gaussian distribution that fits the angle distribution obtained from our Monte Carlo simulations (Fig. 1.2). Specifically, we employ a Gaussian distribution with a mean of 92° and a standard deviation $\sigma = 28^\circ$.

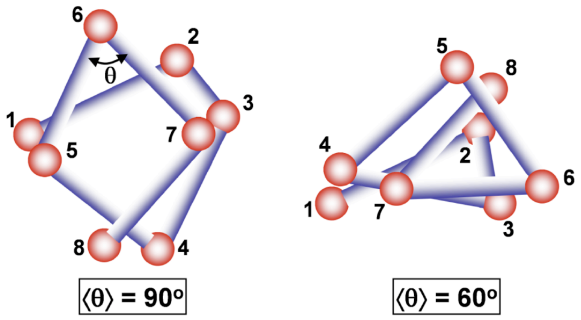

Fig. 1.1: Simplified model of chromatin illustrating the change in internucleosomal interaction pattern from a $(i, i \pm 4)$ to a $(i, i \pm 3)$ when the mean of the input angle distribution changes from 90° to 60°.

We now generate one million configurations of a 12-nucleosome fiber via the above semirandom walk and then compute histograms of internucleosomal distances for nucleosomes i and $i \pm k$ at different values of k. We find that the nucleosome i remains closest to nucleosomes $i \pm 4$ ($k = 4$ curve in Fig. 1.3) when the angle distribution has a mean close to 90°. When the mean angle of the distribution is 60°, the interaction pattern changes such that the closest internucleosomal distance are now between nucleosome i and $i \pm 3$. Changing the mean angle to 0° makes every alternate nucleosome close to each other, as expected.

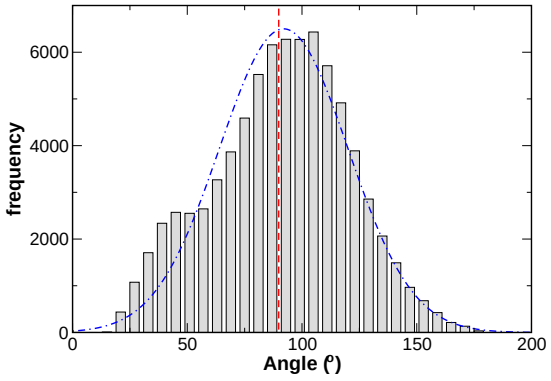

Fig. 1.2: Distribution of angle defined by consecutive nucleosome triplets. The distribution has been averaged over the 22 angles in a 24-unit oligonucleosome. The mean angle of 92° is shown as the vertical red dashed line, and the Gaussian fit to the data is shown by the dotted-dashed blue curve (standard deviation $\sigma = 28^\circ$).

Recall that nucleosomal DNA winds 1.75 times around the nucleosome. This corresponds to a 90° angle subtended between the entry/exit points of linker DNA in our flexible-tail model of oligonucleosomes (5–7). This implies that consecutive nucleosome triplets should subtend an angle of 90° if all interactions between linker DNAs, nucleosome cores, and histone tails are zeroed out. Remarkably, this angle remains

close to 90° even in the presence of energetic interactions in moderately folded chromatin without linker histones. This is because the electrostatic repulsion between the entering/exiting linker DNAs (which tends to expand the mean angle between consecutive nucleosomes) is exactly counterbalanced by the attractive interactions between nucleosomes mediated through the histone tails. The cumulative effect is to maintain the nucleosome triplet angle close to 90°. We speculate that, in highly compact chromatin containing linker histones, the attractive interactions between nucleosomes mediated via the histone tails will dominate the repulsive interactions between linker DNAs and cause the mean angle to decrease from 90°, leading to a different interaction pattern.

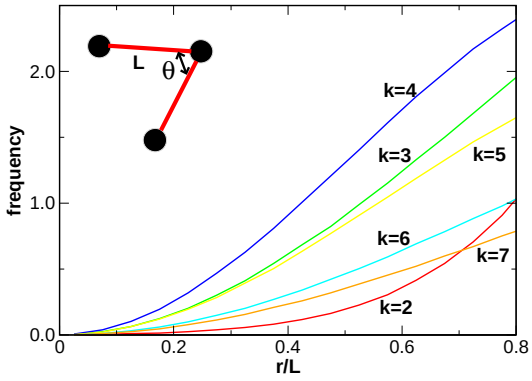

Fig. 1.3: Frequency histogram of internucleosomal distances r (normalized by L, the length of linker DNA) of nucleosome pairs i and $i \pm k$ for $k = 2, \cdots, 7$. The histogram has been obtained for $\theta = 92^\circ$ and $\sigma = 28^\circ$.

Appendix 2: Tail Regrowth—Configurational Bias Monte Carlo

For efficient sampling of histone tail configurations, we employ the configurational bias Monte Carlo (CBMC) method (1–3). This method randomly selects a histone tail and regrows it bead by bead, beginning with the tail bead attached to the nucleosome core, using the Rosenbluth scheme (4).

In the first step of tail regrowth, for the selected tail with N beads, N_t trial positions of the first bead denoted by $\mathbf{r}_{1,j}$, where $j = 1, \cdots, N_t$, are generated. Each position $\mathbf{r}_{1,j}$ is then determined using

$$\mathbf{r}_{1,j} = \mathbf{r}_{1,f} + \mathbf{b}_{1,j}, \tag{1}$$

where $\mathbf{r}_{1,f}$ is the attachment point of the tail bead on the nucleosome core, and $\mathbf{b}_{1,j}$ is a randomly oriented vector whose length is sampled from a Boltzmann distribution corresponding to the potential energy of the spring attaching the tail bead to the core (see ref. 5 for histone tail model). One trial position s is selected with a probability proportional to its Boltzmann weight, i.e.,

$$P(\mathbf{r}_{1,s}) = \frac{\exp(-\beta U_s^{ext})}{w_1}, \quad w_1 = \sum_{j=1}^{N_t} \exp(-\beta U_j^{ext}), \tag{2}$$

where U_j^{ext} is the "external" energy of interaction of the tail bead at position $\mathbf{r}_j$ with the rest of the oligonucleosome, β is the reciprocal temperature ($1/k_BT$), and w_1 is the Rosenbluth factor for the first bead.

Similarly, the position of the second tail bead is obtained by selecting one of the N_t trial positions $\mathbf{r}_{2,j}$ from its Boltzmann's weights, where

$$\mathbf{r}_{2,j} = \mathbf{r}_{1,s} + \mathbf{b}_{2,j}, \tag{3}$$

where $\mathbf{b}_{2,j}$ is a randomly oriented vector whose length is sampled from a Boltzmann distribution corresponding to the stretching energy of the bond. The Rosenbluth factor for this bead, w_2, is recorded. Successive tail beads $k = 3, \cdots, N$ are inserted similarly, but the generated trial bond vectors $\mathbf{b}_{k,j}$ are oriented according to the Boltzmann distribution associated with the bending energy of the bond instead of randomly. The Rosenbluth factors corresponding to each bead insertion, w_k, are recorded.

Once all the beads have been succesfully inserted, the overall Rosenbluth factor for growing the entire chain is calculated: $W_{new} = \prod_{i=1}^{N} w_i$. Using a similar procedure as described above, the old histone tail configuration is *retraced* and its Rosenbluth factor, W_{old}, computed. Note that the selected trial position for bead k, $\mathbf{r}_{k,i}$, is always the old tail position here. The generated histone chain is then accepted with a probability given by

$$P_{acc} = \min[1, W_{new}/W_{old}]. \tag{4}$$

For all simulations, we choose $N_t = 4$ trials and obtain acceptance ratios of about 0.3 (averaged over all tails).

Appendix 3: End-Transfer Configurational Bias Monte Carlo

We have also developed a new method based on the configurational bias Monte Carlo to sample both bonded and nonbonded degrees of freedom of long and complex biopolymers that contain a repeating motif. We call this method *end-transfer configurational bias MC* (EtCBMC). We describe briefly below the method's main concept and its application to the thermodynamic sampling of oligonucleosomes.

For our oligonucleosomes, the repeating motif is a single nucleosome core plus its 10 histone tails and six linker beads. We focus first on the two repeating motifs at the ends of the oligonucleosome. In Fig. 3.1, the two motifs are colored blue and red. The former is denoted as "front" (F) motif, and the latter is the "end" (E) motif. The method selects one of these motifs with a probability $1/2$ and transfers it to the other end with a new configuration. The entire motif is regrown efficiently using the configurational bias approach described in *Appendix 2*, where Rosenbluth weights of the regrown motif at one end of the oligonucleosome and of the "old" motif at the opposite end need to be computed. The end transfer is then accepted with a probability

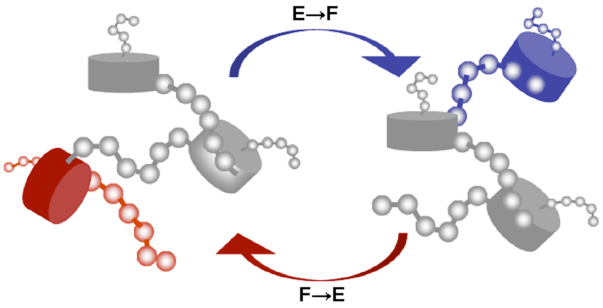

Figure 3.1: Application of EtCBMC method on a tri-nucleosome, highlighting both its $E \rightarrow F$ and $F \rightarrow E$ features. The nucleosome cores are depicted as cylinders and only one histone tail is featured for convenience. The portions of the tri-nucleosome shown in grey are regions conserved during the EtCBMC move while the red and blue shaded regions denote the end and front regions.

$$P_{acc} = \min[1, W_{new}/W_{old}], \tag{5}$$

where W_{new} and W_{old} are the cumulative Rosenbluth weights of regrowing and retracing the histone tails, linker DNA beads, and the nucleosome core of the new and old motifs, respectively. To ensure microscopic reversibility, both the front-to-end ($F \rightarrow E$) and end-to-front ($E \rightarrow F$) moves are attempted with equal probabilities (see Fig. 3.1).

The primary difference between our approach and the traditional CBMC approach is that the motif at one end of the oligonucleosome is regrown at the opposite end rather than at the same end, as in the CBMC approach. This allows an efficient sampling of the entire oligonucleosome (once a sufficient number of $F \rightarrow E$ and $E \rightarrow F$ moves attempted have been accepted). Our method yields an acceptance ratio of 0.1% for high salt conditions, but considerably lower acceptance ratios at low salt conditions where the electrostatic energy landscape is much more rugged. Therefore, we employ the EtCBMC method only for sampling oligonucleosomes at 0.2 M salt. We use $N_t = 10$ trial positions for nucleosome core/DNA linker bead insertion and $N_t = 4$ for histone tail bead insertion.

1. Frenkel, D, Mooij, G. C. A. M, Smit, B. (1992) *J. Phys. Cond. Matter* **4**:3053–3076.
2. de Pablo, J. J, Laso, M, Suter, U. W. (1992) *J. Chem. Phys.* **96**:2395–2403.
3. Frenkel, D, Smit, B. (2002) *Understanding Molecular Simulation: From Algorithms to Applications* (Academic Press, San Diego, CA).
4. Rosenbluth, M. N, Rosenbluth, A. W. (1955) *J. Chem. Phys.* **23**:356–359.
5. Arya, G, Zhang, Q, Schlick, T. (2006) *Biophys. J.* **91**:133–150.
6. Beard, D. A, Schlick, T. (2001) *Structure (London)* **9:**105–114.
7. Sun, J, Zhang, Q, Schlick, T. (2005) *Proc. Natl. Acad. Sci. USA* **102:**8180–8185.